Received: 1 March 2017 | Revised: 12 May 2017 | Accepted: 16 May 2017
DOI: 10.1002/aoc.3924

FULL PAPER

WILEY Applied Organometallic Chemistry

Equisetum arvense As an abundant source of silica nanoparticles. $SiO_2/H_3PW_{12}O_{40}$ nanohybrid material as an efficient and environmental benign catalyst in the synthesis of 2-amino-4H-chromenes under solvent-free conditions

Reza Tayebee[1,2,3] | Akbar Pejhan[4] | Hassan Ramshini[5] | Behrooz Maleki[1] | Nasrin Erfaninia[1] | Zohre Tabatabaie[2,3] | Effat Esmaeili[2,3]

[1] Department of Chemistry, Hakim Sabzevari University, Sabzevar 96179-76487, Iran
[2] Department of Chemistry, Payame Noor University (PNU), Tehran 19395-4697, Iran
[3] Department of Chemistry, Payame Noor University (PNU), Gonabad, Iran
[4] Department of Physiology, Faculty of Medicine, Sabzevar University of Medical Sciences, Sabzevar, Iran
[5] Department of Biology, Payam Noor University, 19395-4697 Tehran, Islamic Republic of Iran

Correspondence
Reza Tayebee, Department of Chemistry, Hakim Sabzevari University, Sabzevar, Iran.
Email:rtayebee@hsu.ac.ir

Akbar Pejhan, Department of Physiology, Faculty of Medicine, Sabzevar University of Medical Sciences, Sabzevar, Iran.
Email: pejhana@medsab.ac.ir

Funding information
Research Councils of Sabzevar University of Medical Sciences; Hakim Sabzevari University

Uniform SiO_2 nanoparticles were successfully prepared from *Equisetum arvense* obtained from the north-east of Iran. Then, surface modification of the extracted nanoparticles was performed with a methanol solution of $H_3PW_{12}O_{40}$ via wet impregnation method. The prepared nanocatalyst was characterized by XRD, FESEM, ICP, UV–Vis, and FT-IR spectroscopy. The supported heterogeneous nanocatalyst was successfully applied as a Lewis/Bronsted acid catalyst in the synthesis of a series of substituted 4H–chromenes via condensation of aromatic aldehydes, malononitrile, and 4-hydroxycoumarin under solventless conditions with fine yields in appropriately short times.

KEYWORDS
4H–coumarins, catalytic, $H_3PW_{12}O_{40}$, heterogeneous, multi-component, nanomaterial, nano-silica

1 | INTRODUCTION

Nano-sized catalysts impetuses keep on attracting enthusiasm for different research areas due to their various physical and chemical properties when contrasted to the bulk material. When, the extremely small-sized particles with expanded surface area expose to the reactant molecules, allowing more interactions to occur simultaneously; therefore, accelerating the reaction. A few methodologies, including sol–gel, thermal procedures and vapor-phase reaction have been unveiled for the preparation of nano-silica. However, the high cost of the synthesis strategies has confined their extensive applications and unquestionably, preparing ultra-fine silica powders with high surface area bring about various technological applications.[1]

Catalysis by heteropolyacids and related compounds is a field of expanding significance in nanocatalysis.[2–4] They are promising applicants for catalyst design due to their controllable redox and acid properties and have been actually utilized in some automated procedures.[5,6] Although diverse neutral or acidic solid supports such as zirconia and active carbon have been resolved to immobilize heteropolyacids, nanoscaled silica materials have been chosen as one of the best supports.

Chromenes are essential oxygenated heterocyclic compounds endowed with different activities for example, antioxidative, antihypertensive, antitumor and antiviral, antidepressant, antileishmanial, antibacterial, diuretic, anticoagulant, anti-tubulin, antiallergenic, and hypotensive activities.[7] Chromenes are well known to activate potassium channels and inhibit dihydrofolate reductases and phosphodiesterase IV and have been utilized as pigments, cosmetics, potential biodegradable agrochemicals, optical brighteners, laser dyes and fluorescence markers.[8–13]

In any case, a couple of methodologies have been accounted for the preparation of these widely exploited pharmacophores which suffer from disadvantages including relying on multistep conditions, utilization of harmful organic solvents or catalysts containing transition metals, tedious work-up, troublesome waste discarding, high reaction time and low yields.[14]

Considering critical preceding properties of chromene derivatives, advancement of useful clean and uncomplicated strategies for the efficient preparation of these compounds by applying accessible reagents under catalytic conditions is of great importance.

Performing organic reactions using solid acid catalysts is associated with different advantages, for example, good agreement with the environment, the appropriate thermal stability of catalyst, catalyst efficiency, product isolation and straightforward process, using mild conditions and reducing the volume of wastes. In continuation of our efforts to probe new and green methodologies based on solid acid catalysts under heterogeneous conditions, [15] a new routine fashion is disclosed for the production of reactive nano-silica from a commonplace plant Field Horsetail (*Equisetum arvense*) which is a Perennial from creeping rhizomes and often forming large colonies which is growing in nutritionally poor soil. The stems of this plant contain more than 10% silica, therefore, can be considered as a suitable environmental benign source of silica. The white ash obtained procure from controlled burning and calcination at generally moderate temperatures creates the main deposit containing silica in the appearance of an amorphous phase.[16–19]

The small tiny particle diameter and high surface area of the supplied nano-silica powders gave rise to heterogenized $H_3PW_{12}O_{40}$ (HPA) to upgrade its catalytic execution. The developed $SiO_2/H_3PW_{12}O_{40}$ nanocatalyst endeavored as an active catalyst in the preparation of different substituted 2-amino-4H-chromenes through contraction of malononitrile, aromatic aldehyde, and 4-hydroxycoumarin under solvent-less-free conditions (Scheme 1).

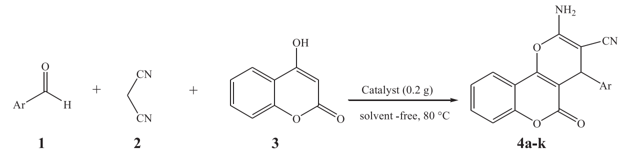

SCHEME 1 General route for the preparation of 2-amino-4H-chromenes

2 | EXPERIMENTAL SECTION

2.1 | Materials and methods

Solvents and beginning materials were purchased from commercial sources and handled as received. Scanning electron micrograph (SEM) pictures were taken by XL-30 Phillips (1992). The crystalline structures of the samples were surveyed by X-ray diffraction (XRD) investigation on a PW1800-PHILIPS diffractometer with Cu K_α radiation ($\lambda = 1.5418$ Å) at 20 keV. FT-IR spectra were recorded on an 8700 Shimadzu spectrophotometer in the area of 400 to 4000 cm^{-1} using KBr pellets. ^1H NMR (300 MHz) spectra were recorded on a Bruker-Avance spectrometer. The chemical composition of the analyzed materials was detected by an inductively coupled plasma (ICP-MS) model Vista-pro and samples were totally dissolved in a sensible hot acid before analysis. A freeze dryer, Model FD-10, Pishtaz Equipment apparatus Engineering Co, Iran, was used for drying of the prepared nanocatalyst. All products were perceived by examination of their physical information with those already announced. $H_3PW_{12}O_{40}$ acid catalyst was set up according to the previously detailed methods.[20]

2.2 | Preparation of Nano-silica from *Equisetum arvense*

The stems of *Equisetum arvense* were washed altogether with water to delete the dissolvable particles or other present contaminants present and substantial impurities like sand. At that point, it was dried in an oven at about 110°C for 24 h. The dried *Equisetum arvense* was refluxed with an acidic solution (0.1 M HCl) under stirring for 90 min. Then, it was cooled and kept around 20 h. Finally, it was isolated and completely washed with hot, refined water until the rinse turned free from acid. The wet solid was subsequently dried in an oven at 110°C for 24 h and designated as *Equisetum arvense*. 20 g of this material was mixed with 160 ml of NaOH (2.5 M) solution. The mixture was heated for 3 h with stirring. It was separated, and the remaining was washed with 40 ml boiling distilled water. The acquired viscous, transparent and colorless solution was permitted to chill off to room temperature. Then, H_2SO_4 (5.0 M) was included under steady stirring at controlled conditions until pH 2, then NH_4OH was added until pH 8.5, and permitted to room temperature for 3 h. Nano silica was prepared by refluxing of the removed silica with HCl (6.0 M) for 4 h; afterward, washed repeatedly with deionized water to make it acid-free. It was then dissolved in stirring NaOH (2.5 M). Thereafter, H_2SO_4 was added until pH 8. The precipitated silica was repeatedly washed with warm deionized water to free it from alkali and was dried at 50°C for 48 h in an oven.

2.3 | Surface modification of nano-silica with $H_3PW_{12}O_{40}$

SiO_2/HPA nanohybrid material was supplied through the well-known wet impregnation strategy. Accordingly, 0.1 g of $H_3PW_{12}O_{40}$ was dissolved in 5 ml methanol. Then, 0.9 g nano-silica was gradually added to the obtained solution during 20 min. At that point, the acquired colloid mixture was stirred at 30°C for 6 h until methanol vanished. The resulting powder was dried at 80°C under air for 24 h. The amount of tungsten in SiO_2/HPA was measured by ICP. For this, 2 ml of 1:1 concentrated HNO_3: $HClO_4$ was added to an exact amount of the nanocomposite in a polyethylene beaker and warmed up to dried. This procedure was repeated three times and afterward 2 ml HF was added and heated to demolish the HPA framework. Eventually, 10 ml diluted HCl was included, and the mixture was warmed for 20 min. The received solution was filtered and diluted in a 50 ml volumetric flask and finally used for the description of tungsten. The content of tungsten in the prepared SiO_2/HPA was 4.4% as determined by ICP analysis. The last analysis demonstrated that ~60% loading of the existing HPA occurred onto the surface of nano-silica. To study the effect of drying conditions on the extent of loaded HPA, the freeze dried nano-silica was prone to the surface modification. Results showed no obvious increment in HPA content for the material prepared under the freeze drying conditions compared with the sample dried under usual thermal conditions.

2.4 | General procedure for the synthesis of substituted 2-amino-4H-chromenes

To a mixture of malononitrile (1 mmol), aromatic aldehydes (1 mmol), and 4-hydroxycoumarin (1 mmol) in a test tube was added SiO_2/HPA nanohybrid material. The resulting mixture was mixed at 80°C; a drop of ethanol was added after solidification of the reaction mixture to maintain liquidity. After fulfillment of the transformation as indicated by TLC, the reaction mixture was cooled to room temperature. Then, chloroform (5 ml) was added, stirred for 1 min, and separated to isolate the heterogeneous catalyst. Eventually, the filtrate was vanished, and the resulting unrefined product was recrystallized from EtOH (96%) to afford the pure product.

2.5 | Spectral data for some selected 2-amino-4H-chromenes

2.5.1 | 2-Amino-4-(phenyl)-3-cyano-4H,5H–pyrano[3,2-c] chromene-5-one (4a)

White solid, mp = 257–259°C. FT-IR (KBr) (ν_{max}/cm^{-1}): 3378, 3286, 3178, 2196, 1709, 1674, 1604. ^1H NMR (300 MHz, DMSO-d_6): δ_H(ppm) 4.46 (1H, s, H-4), 7.25 (2H,d, J = 7.8 Hz, HAr), 7.28 (1H, brs, HAr), 7.33 (2H, t, J = 7.5 Hz, HAr), 7.42 (2H, brs, NH_2), 7.45 (1H, d, J = 8.4 Hz, HAr), 7.49 (1H, t, J = 7.6 Hz, HAr), 7.71 (1H, t, J = 7.5 Hz, HAr), 7.91 (1H, d, J = 7.8 Hz, HAr). ppm.

2.5.2 | 2-Amino-4-(4-cl-phenyl)-3-cyano-4H,5H–pyrano[3,2-c] chromene-5-one (4b)

White solid, mp = 263–265°C. FT-IR (KBr) (ν_{max}/cm^{-1}): 3383, 3314, 3189, 2194, 1715, 1675, 1607. ^1H NMR (300 MHz, DMSO-d_6): δ_H(ppm) 4.50 (1H,s,H-4), 7.31(2H, d, J = 8.2 Hz,HAr), 7.36(2H,brs,NH_2), 7.38 (2H,brs,HAr), 7.44(1H,d, J = 8.2 Hz,HAr), 7.49(1H, t, J = 7.6 Hz, HAr), 7.71(1H,t, J = 7.8 Hz, HAr),7.92 (1H,d, J = 7.8 Hz, HAr) ppm.

2.5.3 | 2-Amino-4-(4-nitrophenyl)-3-cyano-4H,5H–pyrano[3,2-c] chromene-5-one (4e)

Pale Yellow Solid, mp = 251–253°C. FT-IR (KBr) (ν_{max}/cm^{-1}): 3482, 3432, 3371, 3335, 2195, 1718, 1673, 1607, 1506, 1374, 1306. ^1H NMR (300 MHz, DMSO-d_6): δ_H(ppm) 4.68 (1H, s, H-4), 7.47 (1H,d, J = 8.3 Hz, H7), 7.52 (1H, t, J = 7.7 Hz, H9), 7.57 (2H, br s, NH_2),7.60 (2H, d, J = 8.0 Hz, H2,6), 7.74 (1H, t, J = 7.8 Hz, H8), 7.91 (1H, d, J = 7.8 Hz, H10), 8.18 (2H, d, J = 8.3 Hz, H3,5) ppm.

2.5.4 | 2-Amino-4-(3-nitrophenyl)-3-cyano-4H,5H–pyrano[3,2-c] chromene-5-one (4f)

White solid, mp = 258–260°C. FT-IR (KBr) (ν_{max}/cm^{-1}): 3404, 3322, 3194, 2202, 1703, 1672, 1531, 1349 cm^{-1}. ^1H NMR (300 MHz, DMSO-d_6): δ_H(ppm) 4.74 (1H, s, H-4), 7.44 (1H, d, J = 6.7 Hz, H7), 7.51(1H, t, J = 7.6 Hz, H9), 7.56 (2H, br s, NH_2), 7.64 (1H, t, J = 7.6 Hz,H5), 7.73 (1H, dt, J = 7.5, 1.3 Hz, H8), 7.82 (1H, d, J = 6.8 Hz, H2'),7.92 (1H, dd, J = 6.8, 1.2 Hz, H10), 8.12 (1H, dd, J = 8.4, 1.4 Hz, H4'),8.14 (1H, s, H6) ppm.

2.5.5 | 2-Amino-4-(4-MeO-phenyl)-3-cyano-4H,5H–pyrano[3,2-c] chromene-5-one (4 h)

White solid, mp = 236–238°C. FT-IR (KBr) (ν_{max}/cm^{-1}): 3378, 3314, 3190, 2196, 1709, 1672, 1608. ^1H NMR (300 MHz, DMSO-d_6): δ_H(ppm) 3.72 (3H,s,OCH_3), 4.40(1H,s,H-4),6.87(2H,d, J = 8.1 Hz,HAr),7.18 (2H,d, J = 8.1 Hz,HAr), 7.37(2H,brs,NH_2), 7.45(1H, d, J = 8.3 Hz,HAr), 7.49(1H,t, J = 7.8 Hz, HAr),7.70 (1H,t, J = 7.7 Hz, HAr),7.89(1H,d, J = 7.7 Hz, HAr) ppm.

3 | RESULTS AND DISCUSSION

Silica gel is an inorganic amorphous polymer that is built up from the condensation of silicate tetrahedrons utilizing oxygen as the coupling site, giving rise to the siloxane bond (Si-O-Si) and, at last, nanometer-sized particles. The siloxane groups are on the inside of the particles, and the surface is made out of silanol groups (Si-OH). It is well known that solubility of amorphous silica increases in solutions with pH ≥ 10; hence, the amorphous silica contained in the *Equisetum arvense* can be solubilized when treated with a sodium hydroxide solution with the above pH to form dissolvable silicate.[21] Furthermore, when sodium silicate is acidified, a supersaturated solution of $Si(OH)_4$ monomers is shaped. The silica gel is formed is shaped during the gelification of a silica acid solution using applied a polymerization process, which is separated into three phases including monomer polymerization to form particles, particle growth, and particle union in ramified is branched chains that extend throughout the solution and brings about expanding viscosity and formation of a gel.

3.1 | Characterization and physicochemical properties of nano SiO_2/ $H_3PW_{12}O_{40}$

The physicochemical and morphological properties of the supported $SiO_2/H_3PW_{12}O_{40}$ nanocatalyst were explored by means of UV–Vis, SEM, FT-IR, ICP, and XRD. The most informative technique for the examination of the surface interaction amongst $H_3PW_{12}O_{40}$ and nano-SiO_2 are FT-IR and UV–Vis techniques.

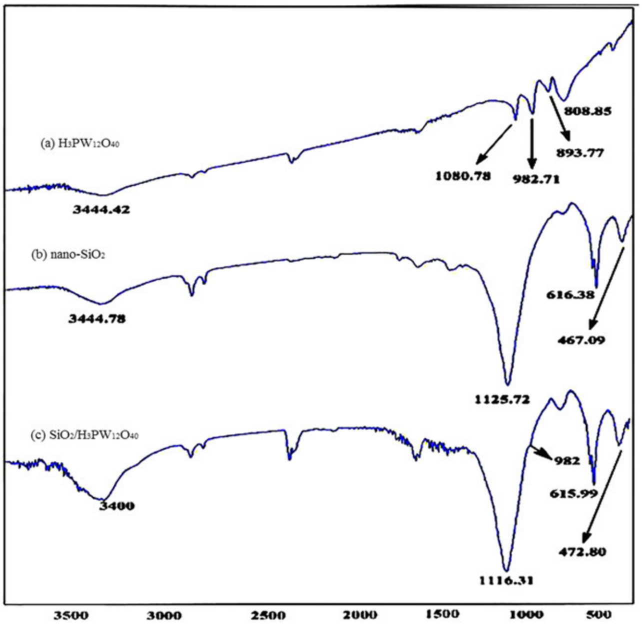

FIGURE 1 FT-IR spectra of free $H_3PW_{12}O_{40}$ (a), nano-SiO_2 (b), and $H_3PW_{12}O_{40}$ impregnated nano-SiO_2 (c)

3.1.1 | FT-IR spectroscopy

FT-IR spectra of the constructed samples in the mid-infrared region from 400 to 1400 cm^{-1} are shown in Figure 1. To ascertain binding of $H_3PW_{12}O_{40}$ onto the surface of nano-SiO_2, FT-IR of all fragments $H_3PW_{12}O_{40}$ (A), nano-SiO_2 (B), and $SiO_2/H_3PW_{12}O_{40}$ (C) were assembled. The bands about 1125 and 616 cm^{-1} in (B) were assigned to the surface O–Si–O bending and Si–O stretching vibrations, respective.[22] The heteropolyacid (A) showed the four characteristic bands in the range 750–1100 cm^{-1}.[23] An expansive around 3420 cm^{-1} represented the vibration of water because of the simple hydration of the materials. The observed bands around 809 and 890 cm^{-1} are due to W-O-W. The peaks around 982 and 1080 cm^{-1} were related to M = O and P-O bonds, individually, which distinctively indicated the neat structure of *Keggin* framework for the heteropolyacid.

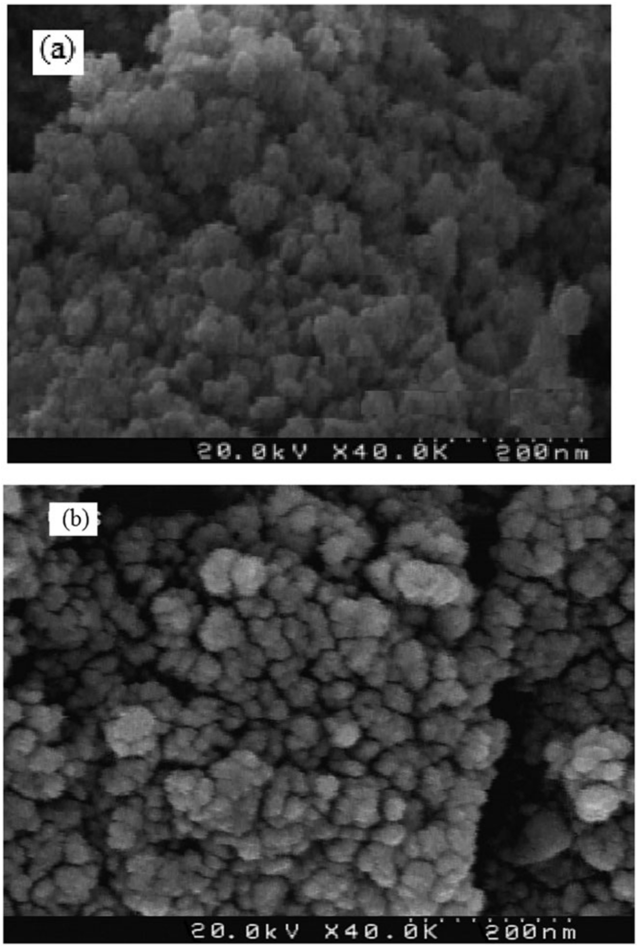

FIGURE 2 The SEM images of nano-SiO_2 (a) and $SiO_2/H_3PW_{12}O_{40}$ nanoparticles (b)

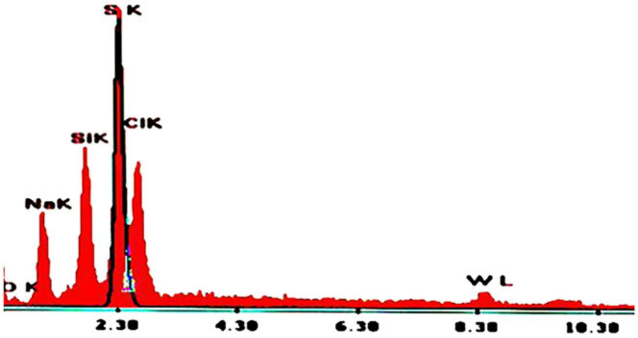

FIGURE 3 EDX spectrum of the prepared $SiO_2/H_3PW_{12}O_{40}$ nanoparticles

Although in the FT-IR of $SiO_2/H_3PW_{12}O_{40}$, these four peaks marginally overlapped with SiO_2, in any case, the peak around 982 cm^{-1} affirmed that the neat perfect structure of the *Keggin* heteropolyacid was preserved after immobilization onto the nano-SiO_2 particles.

3.1.2 | SEM, EDX, and XRD of nano-SiO_2 and $H_3PW_{12}O_{40}$ impregnated nano-SiO_2

The morphology of SiO_2 and SiO_2/HPA nanohybrid catalyst was inspected by SEM as appeared in Figure 2. These micrographs illustrated that the nanoparticles have a semi-spherical morphology with a restricted size distribution with an average diameter of <50 nm. However, functionalization and anchoring of HPA had no critical impact on the structure of nano-SiO_2. The EDX in Figure 3 demonstrated the presence of silica and the heteropolyacid in the prepared nanocomposite. Figure 4 shows X-ray diffractions for commercial nanosilica and for $SiO_2/H_3PW_{12}O_{40}$. Although, the prepared nanosilica seems to behave as amorphous, however, the three weak characteristic signals for nanosilica are observed between 30–40°. The distinct characteristic bands for HPA at 2θ of 28, 31, and 36.2 confirmed that the *Keggin* structure is retained after immobilization.[24]

3.1.3 | UV–vis and ICP analyses

The amount of loaded HPA on nano-SiO_2 was determined by providing UV–Vis spectra of solutions containing HPA during immobilization process. To discover the degree of $H_3PW_{12}O_{40}$ which can be loaded on the support, UV–Vis spectra of solutions containing HPA before and after addition of nano-silica were attained. For this purpose, 0.5 g of SiO_2 was suspended in a 5 ml methanol solution containing 100 mg HPA. Then, the suspension was stirred for 6 h (Figure 5). Clearly, most of the heteropolyacid content (~60%) was adsorbed on the silica surface after 90 min.

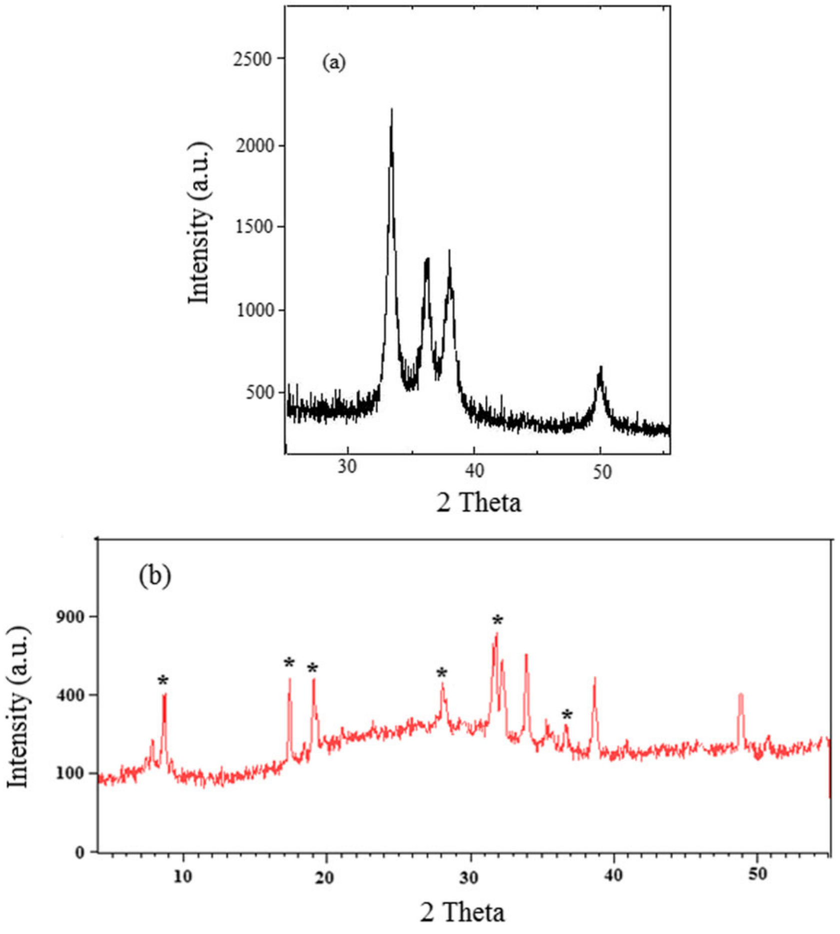

FIGURE 4 X-ray diffraction patterns for commercial nanosilica (a) and $SiO_2/H_3PW_{12}O_{40}$ nanocatalyst (b). Asterisks show heteropolyacid

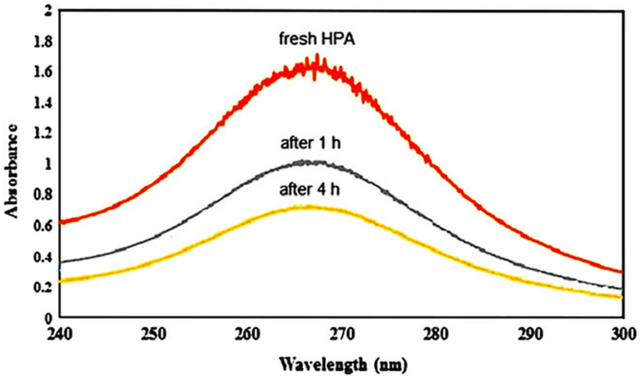

FIGURE 5 UV–vis spectral changes during loading of HPA onto the fabricated nanosilica

TABLE 1 The impact of catalyst amount on the condensation of malononitrile, benzaldehyde, and 4-hydroxycoumarin[a]

Entry	Nano-SiO_2/HPA (g)	Time (min)	Yield (%)[b]
1	0	120	>15
2	0.01	60	30
3	0.03	40	51
4	0.05	30	73
5	0.1	20	82
6	0.2	20	94
7	0.3	20	88

[a] The desired amount of SiO_2/HPA was added to a mixture of malononitrile (1 mmol), benzaldehyde (1 mmol), and 4-hydroxycoumarin (1 mmol). Then, the mixture was stirred at 80 °C in an oil bath and the reaction was followed by TLC. After fulfillment of the reaction, the crude product was purified as depicted in the experimental section.

[b] Isolated yields.

The amount of loaded HPA onto the support was in good concurrence with the result of ICP.

3.2 | Catalytic tests

3.2.1 | Studying the impact of catalyst amount on the condensation reaction

A model reaction was disclosed by applying 0–0.3 g of SiO_2/HPA for the preparation of 2-amino-4H-chromenes (Table 1). Firstly, the reaction was non-beneficial without catalyst and only 15% of product was accomplished after 2 h (entry 1); demonstrating that presence of catalyst was intransitive in the condensation reaction. It was found that 0.01 g of catalyst prompted 30% yield after 60 min (entry 2). This perception established that SiO_2/HPA displayed high catalytic activity in the favorite transformation. The reaction of malononitrile with benzaldehyde and 4-hydroxycoumarin in the presence of 0.2 g catalyst gave the corresponding chromene in 94% yield (Table 1, entry 6). As is expected, yield% was expanded with improving catalyst amount and the greatest yield of 94% was accomplished with 0.2 g of the catalyst after 20 min. However, a higher amount of catalyst brought down yield from 94% to 88% at the same time (entry 7). In this manner, 0.2 g was chosen as the optimal quantity to push the reaction forward.

3.2.2 | Effect of various solvents on the reaction progress

Matching to the fundamental concepts of changing volatile, flammable, and poisonous solvents with less dangerous reaction media, the efficacy of the solvent-free condition was contrasted to the solvent condition in the titled condensation reaction. As a result, condensation of malononitrile with benzaldehyde and 4-hydroxycoumarin was done in various solvents (Table 2). Fortunately, the solvent-free case was found as ideal condition and the best yield was accomplished. In any case, a considerable amount of the intended product was provided in H_2O, EtOH, $CHCl_3$, CH_2Cl_2, and toluene as 84, 78, 33, 20, 60% yields, respectively. Noteworthy, drinking water gave an acceptable result 84% and can be a suitable choice for industrial purposes.

3.2.3 | Effect of reaction temperature and time on the condensation reaction

To enhance the yield and accomplishing the best reaction conditions, the impact of temperature was contemplated on the condensation reaction of malononitrile with benzaldehyde and 4-hydroxycoumarin (Figure 6). As is anticipated, yield was improved with temperature and the best result was acquired at 80°C after 20 min. Also, a further increase in temperature didn't enhance yield. Consequently, the reaction temperature 80°C was kept for all runs.

Effect of reaction time was likewise researched to explore minimum time required to acquire the maximum yield. As Figure 7 shows, 20 min was adequate to acquire 94% yield. No apparent increment in yield was attained after extending reaction time. Conclusively, reactions at various conditions and different molar ratios of substrates in the presence of the heterogeneous $SiO_2/H_3PW_{12}O_{40}$ uncovered that the best

TABLE 2 Effect of various solvents on the condensation of malononitrile, benzaldehyde and 4-hydroxycoumarin[a]

Entry	Solvent	Temp. (°C) (under reflux)	Time (min)	Yield (%)[b]
1	H_2O	100	20	84
2	EtOH	78	20	78
3	$CHCl_3$	61	60	33
4	CH_2Cl_2	40	60	20
5	Toluene	110	30	60
6	-	80	20	94

[a] Reaction conditions are described below Table 1. 0.2 g of the nanocatalyst was used under reflux conditions. 3 ml solvent was used in each case.

[b] Isolated yields.

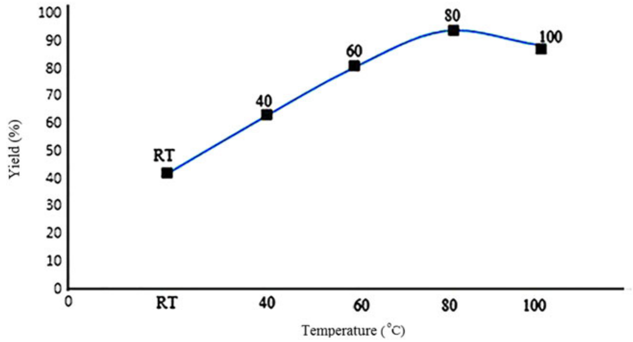

FIGURE 6 Effect of reaction temperature on the condensation of malononitrile, benzaldehyde, and 4-hydroxycoumarin in the presence of 0.2 g of $SiO_2/H_3PW_{12}O_{40}$

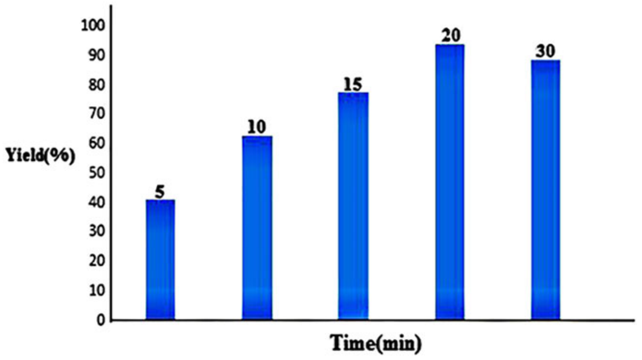

FIGURE 7 Effect of reaction time on the condensation of benzaldehyde, malononitrile, and 4-hydroxycoumarin

TABLE 3 Studying the catalytic activity of different heteropolyacids[a]

Entry	Catalyst	Amount (g)	Time (min)	Yield (%)	Mol (%)
1	$H_3PW_{12}O_{40}$	0.02	20	88	0.7
2	$H_6P_2W_{18}O_{62}$	0.03	20	84	0.7
3	$H_3PMo_{12}O_{40}$	0.01	20	80	0.7
4	$H_5PW_{10}V_{20}O_{40}$	0.02	20	75	0.7

[a] The desired amount of different of HPA was added to a mixture of malononitrile (1 mmol), benzaldehyde (1 mmol) and 4-hydroxycoumarin (1 mmol). Then, the mixture was stirred at 80°C in an oil bath and the reaction was followed by TLC. After completion of the reaction, the crude product was purified as described in the experimental part.

condition was solvent-free at 80°C in the presence of 0.2 g of the nanocatalyst.

3.2.4 | Comparison of the catalytic activities of different heteropolyacids

Catalytic activities of $H_3PW_{12}O_{40}$, $H_6P_2W_{18}O_{62}$, $H_3PMo_{12}O_{40}$ and $H_5PW_{10}V_{20}O_{40}$ were compared in the desired condensation reaction (Table 3). Although, all of the examined catalysts were successful and provided 75–88% yield after 20 min, however, the first showed the best yield. Many variables for example, acidity of the heteropolyacid, negative charge density speared over oxygen atoms, structural composition distortions, and approach of the substrate molecule into the bulk of the heteropolyacid would contribute to the catalytic efficiency of the examined heteropolyacids under the reaction conditions.

3.2.5 | Studying generality of the desired condensation reaction

Since, pharmacological and biological activities of chromenes depend on the nature of substituents being either on the 4H–pyran or on the adjacent rings, extension and generality of the present methodology were assessed by applying the condensation reaction under the achieved perfect conditions with different aromatic aldehydes bearing different substituents (Table 4). Selective and efficient generation of a variety of chromenes with the assembled nano-hybrid catalyst was studied by considering the condensation reaction under the optimized conditions by using different aromatic aldehydes bearing electron withdrawing (donating) groups and halogen-substituted counterparts. Table 4 shows most of the electron-rich and electron-poor aromatic aldehydes reacted well and produced high yields. Aromatic aldehydes including electron-withdrawing groups gave the respective addition excess, products in good yields; while, the others containing electron-donating groups afforded moderate yields.

3.2.6 | Comparison of the viability of the present approach with some reported protocols

The productivity of the $SiO_2/H_3PW_{12}O_{40}$ catalytic system was contrasted to some reported catalysts for the synthesis of 2-amino-4H-chromenes. The reaction of malononitrile with benzaldehyde and 4-hydroxycoumarin was chosen in the presence of different catalysts as organized in Table 5. Clearly, $SiO_2/H_3PW_{12}O_{40}$ is more effective compared to the reported catalysts respecting the yield. Likewise, the present methodology employed a low cost and easily prepared catalyst under solvent-free conditions. Albeit, a portion of the introduced catalysts pushed the reaction even though at better reaction conditions, nonetheless, they needed costly and harmful reagents and solvents and higher amounts of catalyst. The present catalytic framework conveys distinct advantages in competition with the already revealed strategies; regarding yield, straightforward work-up, mild reaction conditions and lack of toxicity.

3.2.7 | Studying stability and reusability of nano-$SiO_2/H_3PW_{12}O_{40}$

Comparison of the infrared spectra of nano-$SiO_2/H_3PW_{12}O_{40}$ before and after condensation reaction (regenerated after 5 runs) and observation of the characteristic bands around 800–1100 cm^{-1} clearly confirmed preservation of the Keggin

TABLE 4 Synthesis of different substituted chromenes in the presence in the nearness of SiO_2/HPA under solvent-free conditions[a]

Entry	Ar-	Time (min)	Yield (%)[b]	M.p.(°C)[c]	Lit. M.p. (°C)	Ref
4a	Phenyl	20	94	257–259	[256–258]	[14e]
4b	4-Cl-phenyl	15	91	263–265	[262–264]	[14e]
4c	2-Cl- phenyl	22	88	265–267	[266–268]	[14a]
4d	4-Me- phenyl	25	90	254–256	[254–255]	[14a]
4e	4-NO_2- phenyl	20	89	251–253	[252–254]	[14e]
4f	3-NO_2- phenyl	30	86	258–260	[260–262]	[14e]
4 g	3-MeO- phenyl	25	87	244–245	[241–243]	[14e]
4 h	4-MeO- phenyl	25	88	236–238	[238–240]	[14e]
4i	4-$N(CH_3)_2$–phenyl	20	89	224–226	[220–222]	[14e]
4j	4-F-phenyl	20	92	260–262	[260–262]	[14a]
4 k	3-Cl-phenyl	20	85	244–246	[246–248]	[14j]

[a] Reaction conditions are described below Table 1.

[b] Yields refer to the separated pure products. The desired pure products were described by comparison of their physical information with those of known compounds.

[c] Melting points are uncorrected and refer to the desired products.

TABLE 5 Comparison of the efficacy of nano-$SiO_2/H_3PW_{12}O_{40}$ with some catalysts for the synthesis of 2-amino-4-(phenyl)-3-cyano-4H,5H–pyrano[3,2-c] chromene-5-one (4a)

Entry	Catalyst and conditions	Time(min)	Yield (%)	Ref
1	In this work	20	94	--
2	Triethylbenzylammonium chloride (TEBA), H_2O, 90 °C	480	95	[14a]
3	*o*-Benzenedisulfonimide (OBS), solvent-free, 120 °C	50	85	[14e]
4	Hexamethylenetetramine, EtOH/reflux	15	92	[14f]
5	[Fe_2O_3@ HAp Si $(CH_2)_3$-AMP], H_2O, reflux	10	78	[14g]
6	Sodium dodecyl sulfate (SDS), H_2O, 60 °C	120	85	[14j]
7	NaBr, electrolysis, EtOH, 60 °C	60	92	[14k]

structure (Figure 8). What's more, to guarantee reproducibility of the condensation reaction, repeated repetitious typical experiments were performed under same reaction conditions. The acquired yields were found to be reproducible within ±3% variation.

Reproducibility and reusability of nano-$SiO_2/H_3PW_{12}O_{40}$ were examined in the synthesis of 2-amino-4H-chromenes, as appeared in Figure 9. After fulfillment of the primary run, chloroform was added and the catalyst, as the sole insoluble material, was recovered from the reaction by filtration. The separated catalyst was totally washed with chloroform; then, dried and tested in another run. The catalyst was tried for subsequent five runs. Very good reusability was watched for the catalyst.

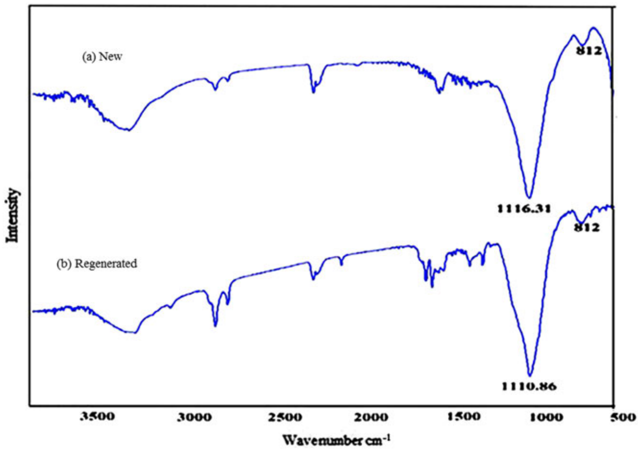

FIGURE 8 FT-IR spectra of new (a) and regenerated (b) $SiO_2/H_3PW_{12}O_{40}$

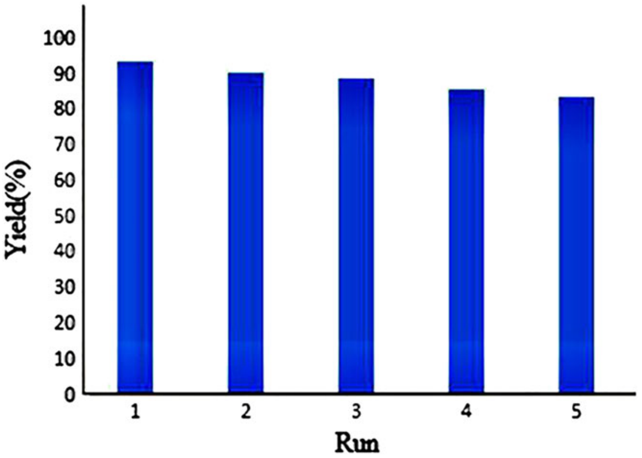

FIGURE 9 Yield% as a function of reusability of $SiO_2/H_3PW_{12}O_{40}$

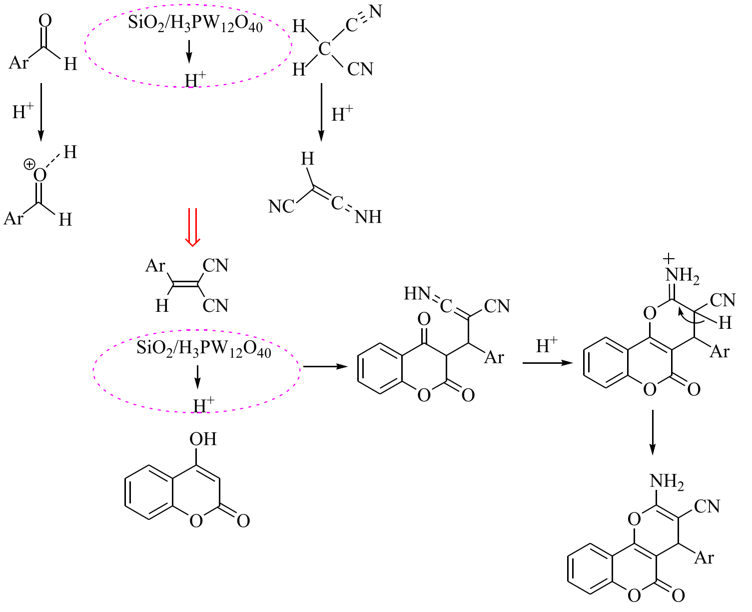

SCHEME 2 Proposed route for the synthesis 2-amino-4H-chromenes

3.2.8 | Hot filtration test

A hot filtration test was arranged to be sure that the catalytic activity of the nanohybrid catalyst was originated from the conjugated composite SiO$_2$/HPA and not from the drained segments, especially H$_3$PW$_{12}$O$_{40}$, in the reaction mixture. Thus, to a mixture of malononitrile (1 mmol), aldehyde (1 mmol), and 4-hydroxycoumarin (1 mmol) was added 0.02 g of SiO$_2$/H$_3$PW$_{12}$O$_{40}$ and the reaction was started as depicted in the experimental part for 10 min. At this stage, the product yield was 63%. At that point, hot chloroform was added and the catalyst was separated off and with the filtrate, the reaction proceeded for another 10 min at 80°C. Yield% was enhanced to 67%; consequently, no significant increase was observed. This obviously affirmed the satisfactory steadiness of nano-SiO$_2$/HPA in the condensation reaction and no significant destruction of the catalyst over the span of the reaction. This result was furthermore asserted by reproducibility and reusability investigations of the catalyst as specified previously.

3.2.9 | Suggesting a plausible reaction pathway

The reaction is anticipation to proceed via the Knoevenagel condensation of an aromatic aldehyde with malononitrile. This step can be catalyzed by SiO$_2$/H$_3$PW$_{12}$O$_{40}$ via the elimination of an acidic hydrogen from the active nitrile and formation of an intermediate nitrile. In a model reaction, the knoevenagel condensation of malononitrile and benzaldehyde was performed and the produced intermediate was separated (mp. 81–82°C).[14h] Then, the Michael-type addition of the 4-hydroxycoumarin with the Knoevenagel intermediate gave rise to the in situ formation of benzylidinemalononitrile. Thereafter, intramolecular nucleophilic cyclization (Thorpe–Ziegler type reaction) and tautomerization of this intermediate afforded the final product (Scheme 2).[14d, g–h] It is plausible to consider both Lewis/ Bronsted acid functions for the nanocatalyst, which activates both carbonyl group of aldehyde and increases nucleophilic attributes of malononitrile on the other.

4 | CONCLUSION

The amorphous nano-silica powder was prepared with the small grain size, expansive surface area, and high degree of purity from *Equisetum arvense*. Then, SiO$_2$/H$_3$PW$_{12}$O$_{40}$ was incorporated by the impregnation strategy and the prepared nanocatalyst was characterized and used as a powerful and reusable strong solid acid catalyst in the synthesis of 2-amino-4H-chromenes under solvent-free conditions. According to SEM, the mean grain size of about 50 nm was estimated. FT-IR of SiO$_2$/H$_3$PW$_{12}$O$_{40}$ exhibited that the primary *Keggin* structure of the loaded heteropolyacid was preserved after supporting onto SiO$_2$. The entire synthetic sequence possesses convenient generality, is cost-effective and environmentally friendly, which made the method honorable as a reliable contribution to the current procedures in the field of 2-amino-4H-chromenes synthesis. This safe and clean method would be an acceptable applicant for the automated applications.

ACKNOWLEDGEMENTS

Partial financial support from the Research Councils of Sabzevar University of Medical Sciences and Hakim Sabzevari University is greatly appreciated.

REFERENCES

[1] L. Sun, K. Gong, *Ind. Eng. Chem. Res.* **2001**, *40*, 5861.

[2] I. V. Kozhevnikov, *J. Mol. Catal. A: Chem.* **2001**, *305*, 104.

[3] T. Okuhara, *Chem. Rev.* **2002**, *102*, 3641.

[4] U. Kortz, A. Muller, J. Slageren, J. Schnack, N. S. Dalol, M. Dressel, *Coord. Chem. Rev.* **2009**, *253*, 2315.

[5] M. Misono, *Chem. Commun.* **2001**, *13*, 1141.

[6] J. S. Min, N. Mizuno, *Catal. Today* **2001**, *71*, 89.

[7] M. Curini, G. Cravotto, F. Epifano, G. Giannone, *Curr. Med. Chem.* **2006**, *13*, 199.

[8] G. A. Kraus, I. Kim, *J. Org. Chem.* **2003**, *68*, 4517.

[9] J. G. Tangmouo, A. L. Meli, J. Komguem, V. Kuete, F. N. Ngounou, D. Lontsi, V. P. Beng, M. I. Choudhary, B. L. Sondengam, *Tetrahedron Lett.* **2006**, *47*, 3067.

[10] (a) R. O. S. Kitamura, P. Romoff, M. C. M. Young, M. J. Kato, J. H. G. Lago, *Phytochemistry* **2006**, *67*, 2398. (b) F. Borges, F. Roleira, N. Milhazes, L. Santana, E. Uriarte, *Curr. Med. Chem.* **2005**, *12*, 887.

[11] F. Chimenti, B. Bizzarri, A. Bolasco, D. Secci, P. Chimenti, S. Carradori, A. Granese, D. Rivanera, D. Lilli, M. M. Scaltrito, M. I. Brenciaglia, *Eur. J. Med. Chem.* **2006**, *41*, 208.

[12] D. R. Anderson, S. Hegde, E. Reinhard, L. Gomez, W. F. Vernier, L. Lee, S. Liu, A. Sambandam, P. A. Snider, L. Masih, *Bioorg. Med. Chem. Lett.* **2005**, *15*, 1587.

[13] M. V. Kulkarni, G. M. Kulkarni, C. H. Lin, C. M. Sun, *Curr. Med. Chem.* **2006**, *13*, 2795.

[14] (a) J. Wang, D. Q. Shi, Q. Y. Zhuang, X. S. Wang, H. W. Hu, *J. Chem. Res.* **2004**, *12*, 818. (b) J. M. Khurana, B. Nand, P. Saluja, *Tetrahedron* **2010**, *66*, 5637. (c) M. G. Dekamin, M. Eslami, A. Maleki, *Tetrahedron* **2013**, *69*, 1074. (d) K. Niknam, A. Jamali, *A. Chin. J. Catal.* **2012**, *33*, 1840. (e) B. Maleki, *Org. Prep. Proced. Int.* **2016**, *48*, 303. (f) H. J. Wang, J. Lu, Z. H. Zhang, *Monatsh. Chem.* **2010**, *141*, 1107. (g) M. Khoobi, L. Ma'mani, F. Rezazadeh, Z. Zareie, A. R. Foroumadi, A. Ramazani, A. Shafiee, *J. Mol. Catal. A: Chem.* **2012**, *359*, 74. (h) H. R. Shaterian, M. Arman, F. Rigi, *J. Mol. Liq.* **2011**, *158*, 145. (i) K. Tabatabaeian, H. Heidari, M. Mamaghani, N. O. Mahmoodi, *Appl. Organometal. Chem.* **2012**, *26*, 56. (j) H. Mehrabi, H. Abusaidi, *J. Iran. Chem. Soc.* **2010**, *7*, 890. (k) Z. Vafajoo, H. Veisi, M. T. Maghsoodlou, H. Ahmadian, *C. R. Chim.* **2014**, *17*, 301.

[15] (a) B. Maleki, S. Barat Nam Chalaki, S. Sedigh Ashrafi, E. Rezaei Seresht, F. Moeinpour, A. Khojastehnezhad, R. Tayebee, *Appl. Organometal. Chem.* **2015**, *29*, 290. (b) B. Maleki, S. Babaee, R. Tayebee, *Appl. Organometal. Chem.* **2015**, *29*, 408. (c) R. Tayebee, M. Jarrahi, B. Maleki, M. K. Razi, Z. B. Mokhtari, S. M. Baghbanian, *RSC Adv.* **2015**, *5*, 10869. (d) B. Maleki, M. Baghayeri, S. A. J. Abadi, R. Tayebee, A. Khojastehnezhad, *RSC Adv.* **2016**, *6*, 96644. (e) B. Maleki, N. Nasiri, R. Tayebee, A. Khojastehnezhad, H. A. Akhlaghi, *RSC Adv.* **2016**, *6*, 79128. (f) R. Tayebee, M. M. Amini, H. Rostamian, A. Aliakbari, *Dalton Trans.* **2014**, *43*, 1550.

[16] S. Huang, S. Jing, J. Wang, Z. Wang, Y. Jin, *J. Powder Technol.* **2001**, *117*, 232.

[17] E. S. M Seo, M. Andreoli, R. Chiba, *J. Mater. Process. Technol.* **2003**, *141*, 351.

[18] T.-H. Liou, *J. Mater. Sci. Eng. A* **2004**, *364*, 313.

[19] N. Yalc, V. Sevinc, *J. Ceram.* **2001**, *27*, 219.

[20] M. M. Heravi, B. Alimadadi Jani, F. Derikvand, H. A. Oskooie, *Catal. Commun.* **2008**, *10*, 272.

[21] U. Kalapathy, A. S. Proctor, A. J. Shultz, *J. Bioresour. Technol.* **2002**, *85*, 285.

[22] Y. Kong, H. Zhu, G. Yang, X. Guo, W. Hou, Q. Yan, M. Gu, C. Hu, *J. Adv. Funct. Mater.* **2004**, *14*, 816.

[23] P. Van Der Voort, M. White, M. Mitchell, A. Verberckmoes, E. Vansant, *Spectrochim. Acta Mol. Biomol.* **1997**, *53*, 2181.

[24] B. M. Devassy, F. Lefebvre, S. B. Halligudi, *J. Catal.* **2005**, *231*, 1.

How to cite this article: Tayebee R, Pejhan A, Ramshini H, et al. *Equisetum arvense* As an abundant source of silica nanoparticles. $SiO_2/H_3PW_{12}O_{40}$ nanohybrid material as an efficient and environmental benign catalyst in the synthesis of 2-amino-4H-chromenes under solvent-free conditions. *Appl Organometal Chem*. 2017;e3924. https://doi.org/10.1002/aoc.3924